The collision energy effect on the stereodynamics of the Ca + HCl→CaCl + H reaction*

Wang Li-Zhi(王立志)[a)b)], Yang Chuan-Lu(杨传路)[b)†], Liang Jing-Juan(梁景娟)[a)], Duan Li-Li(段莉莉)[a)], and Zhang Qing-Gang(张庆刚)[a)]

[a)] College of Physics and Electronics, Shandong Normal University, Jinan 250014, China
[b)] School of Physics and Optoelectronic Engineering, Ludong University, Yantai 264025, China

(Received 13 July 2012; revised manuscript received 7 September 2012)

The stereodynamics of the reaction of Ca + HCl are calculated at three different collision energies based on the potential energy surface [Verbockhaven G *et al*. 2005 *J. Chem. Phys*. **122** 204307] using quasi-classical trajectory theory. The polarization-dependent differential cross sections (PDDCSs) $(2\pi/\sigma)(\mathrm{d}\sigma_{00}/\mathrm{d}\omega_t)$, $(2\pi/\sigma)(\mathrm{d}\sigma_{20}/\mathrm{d}\omega_t)$, $(2\pi/\sigma)(\mathrm{d}\sigma_{22+}/\mathrm{d}\omega_t)$, $(2\pi/\sigma)(\mathrm{d}\sigma_{21-}/\mathrm{d}\omega_t)$ and the distributions of $P(\theta_r)$, $P(\phi_r)$, and $P(\theta_r,\phi_r)$ are calculated. The results indicate that the rotational polarization of the CaCl product presents different characteristics for the different collision energies, and the effects of the collision energy on the vector potential, including the alignment, orientation, and PDDCSs, are not obvious.

Keywords: stereodynamics, quasi-classical trajectory, vector correlation, collision energies effect

PACS: 31.15.Ap, 34.50.Lf, 31.15.Xv **DOI:** 10.1088/1674-1056/22/4/043101

1. Introduction

Recently, with the rapid development of reaction dynamics for computing product angular momentum polarization, research into stereodynamics has been predicted to provide valuable information in understanding the elementary reaction. A number of quasi-classical trajectory (QCT), time-independent quantum dynamics, and time-dependent wave packet calculations have been carried out to explore the collision reaction processes over the last two years.[1–8]

Being a typical reaction of the "Harpoonlike" model mechanism,[9] the Ca + HCl reaction that involves an alkali-earth atom and a hydrogen halide has been considered to analyze the influences of the initial state on the reactants and the final state distribution. Moreover, the reactions $M + HX \rightarrow MX + H$ (M = Be, Mg, Ca, Sr, Ba; X = F, Cl, Br, I) show interesting dynamical features, and many studies of this reaction family have been performed theoretically and experimentally.[10–25] Experimental research into the reaction dynamics of this system has been conducted by photon excitation of the Ca atom in the Ca(1S)–HCl van der Waals complex. However, the CaCl product was initially not detected in its electronic ground state[26–28] because its detection is particularly difficult. Fortunately, Visticot *et al*.[29] detected the Ca–HCl complex by observing the fluorescence of the CaCl molecule in a supersonic beam/laser-ablation experiment. In the theoretical aspect, in 2005, Verbockhaven *et al*.[30] reported on a new *ab initio* PES computed using a coupled cluster method with single and double excitations and perturbative triples (CCSD(T)) and multi-reference configuration-interaction (MRCI) wave functions. This PES is reliable because the results based on the quantum-dynamics calculation and the new surface are in agreement with the experimental data, which describes the full reaction from the Ca + HCl reactant to the CaCl + H product.

As far as we know, most of the studies in the previous work on the Ca + HCl reaction mainly focus on the scalar properties, such as rate constant, cross section, and product population distribution.[30] However, there are few reports about the chemical reaction stereodynamics. Wang *et al*.[31,32] studied the vector properties of the products and investigated the variation in the rotational alignment for the Ca + HCl action by QCT calculations on the PES developed by Verbockhaven *et al*.,[30] and they found that the isotopic effect and the influence of reagent vibration play an important role in determining the stereodynamics of the Ca + HCl reaction and its isotope reactions. To obtain the whole picture of the emerging scattering dynamics, we present the influence of the collision energy on the stereodynamics for the Ca + HCl→CaCl + H reaction in this paper.

2. Theory

2.1. Product rotational polarization

The theory of product rotational polarization applied here is one established in Refs. [33]–[39]. The reference frame is shown in Fig. 1. The reagent relative velocity vector $\boldsymbol{k}$ is parallel to the z axis, and the x–z plane is the scattering plane con-

*Project supported by the National Natural Science Foundation of China (Grant Nos. 11174117, 10974078, 11274205, 11274206, 11147026, and 31200545).
†Corresponding author. E-mail: scuycl@gmail.com
© 2013 Chinese Physical Society and IOP Publishing Ltd

taining the initial and final relative velocity vectors, $\boldsymbol{k}$ and $\boldsymbol{k}'$. The θ_t angle is the angle between the reagent relative velocity and product relative velocity (the so-called scattering angle). The θ_r and ϕ_r angles are the polar and azimuthal angles of the final rotational angular momentum $\boldsymbol{j}'$.

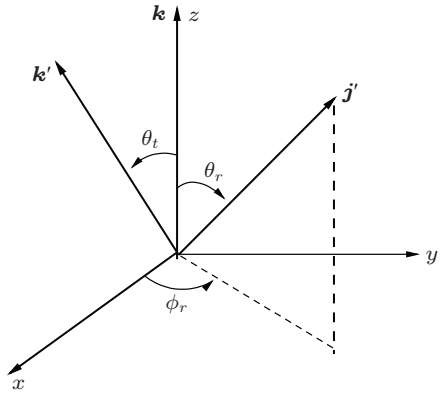


Fig. 1. Center-of-mass coordinate system used to describe the $\boldsymbol{k}$, $\boldsymbol{k}'$, and $\boldsymbol{j}'$ correlations.

A simple way to express the degree of polarization of $\boldsymbol{j}'$ is to use the center-of-mass (CM) frame orientation and alignment parameters. The distribution of the angular momentum $\boldsymbol{j}'$ of the product molecule is described by a function $f(\theta_r)$, where θ_r is the angle between $\boldsymbol{j}'$ and $\boldsymbol{k}$ (the reagent relative velocity vector). Function $f(\theta_r)$ can be represented by the Legendre polynomial as follows:

$$f(\theta_r) = \sum a_n \mathrm{P}_n(\cos\theta_r), \tag{1}$$

where $n = 2$ indicates the product rotational alignment

$$\left\langle \mathrm{P}_2(\boldsymbol{j}'\cdot\boldsymbol{k})\right\rangle = \frac{1}{2}\left\langle 3\cos^2\theta_r - 1\right\rangle. \tag{2}$$

Here, P_2 is the second Legendre moment, and the brackets indicate an average over the distribution of $\boldsymbol{j}'$ about $\boldsymbol{k}$. In the present work, we only calculate the rotational alignment parameter of the product, since it has been solely measured in most of the experiments until now.

Usually, two vector correlations ($\boldsymbol{k}$–$\boldsymbol{j}'$, $\boldsymbol{k}$–$\boldsymbol{k}'$ or $\boldsymbol{k}'$–$\boldsymbol{j}'$) can be expanded into a series of Legendre polynomials. The distribution function $P(\theta_r)$ describing the $\boldsymbol{k}$–$\boldsymbol{j}'$ correlation can be expanded in a series of Legendre polynomials as[33–35]

$$P(\theta_\mathrm{r}) = \frac{1}{2}\sum_k (2k+1)a_0^{(k)}\mathrm{P}_k(\cos\theta_r), \tag{3}$$

where

$$a_0^{(k)} = \int_0^\pi P(\theta_r)\mathrm{P}_k(\cos\theta_r)\sin\theta_r \mathrm{d}\theta_r = \left\langle \mathrm{P}_k(\cos\theta_r)\right\rangle. \tag{4}$$

The expanding coefficient $a_0^{(k)}$ is called the orientation parameter when k is odd, and the alignment parameter when k is even.

The dihedral angle distribution function $P(\phi_r)$ describing the $\boldsymbol{k}$–$\boldsymbol{k}'$–$\boldsymbol{j}'$ correlation can be expanded in the Fourier series as

$$P(\phi_r) = \frac{1}{2\pi}\left(1 + \sum_{\mathrm{even},n\geq 2} a_n\cos n\phi_r\right) + \sum_{\mathrm{odd},n\geq 1} b_n \sin\phi_r, \tag{5}$$

where

$$a_n = 2\langle\cos n\phi_r\rangle, \tag{6}$$

$$b_n = 2\langle\sin n\phi_r\rangle. \tag{7}$$

In this calculation, $P(\phi_r)$ is expanded up to $n = 24$, which shows good convergence. The joint probability density function of angles θ_r and ϕ_r, which defines the direction of $\boldsymbol{j}'$, can be written as

$$\begin{aligned} & P(\theta_r,\phi_r) \\ = & \frac{1}{4\pi}\sum_{kq}[k]a_q^k C_{kq}(\theta_r,\phi_r)^* \\ = & \frac{1}{4\pi}\sum_k\sum_{q\geq 0}[a_{q\pm}^k\cos q\phi_r - a_{q\mp}^k\sin q\phi_r]C_{kq}(\theta_r,0). \end{aligned} \tag{8}$$

In this calculation, the polarization parameter is evaluated as

$$a_{q\pm}^k = 2\langle C_{k|q|}(\theta_r,0)\cos q\phi_r\rangle, \quad \text{when } k \text{ is even;} \tag{9}$$

$$a_{q\mp}^k = 2\mathrm{i}\langle C_{k|q|}(\theta_r,0)\cos q\phi_r\rangle, \quad \text{when } k \text{ is odd.} \tag{10}$$

In the calculation, $P(\theta_r,\phi_r)$ is expanded up to $k = 7$, which is sufficient for good convergence.

The full three-dimensional angular distribution associated with the $\boldsymbol{k}$–$\boldsymbol{k}'$–$\boldsymbol{j}'$ correlation can be represented by a set of generalized polarization-dependent differential cross sections (PDDCSs) in the CM frame. The fully correlated CM angular distribution is written as

$$P(\omega_t,\omega_r) = \sum_{kq}\frac{[k]}{4\pi}\frac{1}{\sigma}\frac{\mathrm{d}\sigma_{kq}}{\mathrm{d}\omega_t}C_{kq}(\theta_r,\phi_r)^*, \tag{11}$$

where $[k] = 2k+1$, $(\sigma^{-1})(\mathrm{d}\sigma_{kq}/\mathrm{d}\omega_t)$ is a generalized PDDCS, and $\sigma^{-1}\cdot(\mathrm{d}\sigma_{kq}/\mathrm{d}\omega_t)$ yields $\sigma^{-1}\cdot(\mathrm{d}\sigma_{k0}/\mathrm{d}\omega_t) = 0$, when k is odd,

$$\frac{1}{\sigma}\frac{\mathrm{d}\sigma_{kq+}}{\mathrm{d}\omega_t} = \frac{1}{\sigma}\frac{\mathrm{d}\sigma_{kq}}{\mathrm{d}\omega_t} + \frac{1}{\sigma}\frac{\mathrm{d}\sigma_{k-q}}{\mathrm{d}\omega_t} = 0, \tag{12}$$

when k is even, q odd or, k is odd, q even,

$$\frac{1}{\sigma}\frac{\mathrm{d}\sigma_{kq-}}{\mathrm{d}\omega_t} = \frac{1}{\sigma}\frac{\mathrm{d}\sigma_{kq}}{\mathrm{d}\omega_t} - \frac{1}{\sigma}\frac{\mathrm{d}\sigma_{k-q}}{\mathrm{d}\omega_t} = 0, \tag{13}$$

when k is even, q even or, k is odd, q odd.

Many photon-initiated bimolecular reaction experiments will be sensitive to only those polarization moments with $k = 0$ and $k = 2$. In order to compare the calculations with experiments, $(2\pi/\sigma)(\mathrm{d}\sigma_{00}/\mathrm{d}\omega_t)$, $(2\pi/\sigma)(\mathrm{d}\sigma_{20}/\mathrm{d}\omega_t)$, $(2\pi/\sigma)(\mathrm{d}\sigma_{22+}/\mathrm{d}\omega_t)$, $(2\pi/\sigma)(\mathrm{d}\sigma_{21-}/\mathrm{d}\omega_t)$ are calculated. In the above calculations, PDDCSs are expanded up to $k_1 = 7$, which is sufficient for good convergence.

2.2. Computational details of QCT

To shed more light on the vector correlations of the reaction of Ca + HCl→CaCl + H, we describe quasi-classical trajectory (QCT) calculations at different collision energies (E_T = 0.6, 0.8, and 1.0 eV) to study the stereodynamics of the title reaction. The QCT calculations have been performed using a code developed in Refs. [34]– [39]. The vibrational and rotational levels of the reactant molecule are taken to be $v = 0$ and $j = 0$, respectively. The accuracy of the numerical integration is verified by checking the conservations of the total energy and total angular momentum for every trajectory. In our calculation, a batch of 10^5 trajectories are run for each reaction and the integration step size is chosen to be 0.1 fs.

3. Results and discussion

The calculated distribution of $P(\theta_r)$ of the product, which describes the $\boldsymbol{k}$–$\boldsymbol{j}'$ correlation, is related to the collision energy. Figure 2 shows that the peak of $P(\theta_r)$ distribution is at $\theta_r = 90^\circ$ and symmetric with respect to 90°, which suggests that $\boldsymbol{j}'$ is strongly aligned along the direction at right angles to $\boldsymbol{k}$. It is clear that there is a small discrepancy between the distributions of $P(\theta_r)$ of the title reaction at three collision energies. The peak of $P(\theta_r)$ becomes higher with the collision energy increasing from 0.6 eV to 0.8 eV, implying that the product rotational alignment becomes stronger. A simple way to express the degree of product rotational polarization is to use the center-of-mass frame alignment parameter $\langle P_2(\boldsymbol{j}' \cdot \boldsymbol{k})\rangle$. As is well known, $\langle P_2(\cos\theta)\rangle$ is very important because when the value is close to −0.5, suggesting that $\boldsymbol{j}'$ is preferentially polarized and perpendicular to the reagent relative velocity, it is obviously seen that our calculated values of $\langle P_2(\boldsymbol{j}' \cdot \boldsymbol{k})\rangle$ shown in Table 1 are consistent with the distributions of $P(\theta_r)$.

Table 1. Values of product rotational alignment parameter $\langle P_2(\boldsymbol{j}' \cdot \boldsymbol{k})\rangle$ calculated at three collision energies.

Collision energy	0.6 eV	0.8 eV	1.0 eV
$\langle P_2(\boldsymbol{j}' \cdot \boldsymbol{k})\rangle$	–0.493932	–0.495977	–0.496656

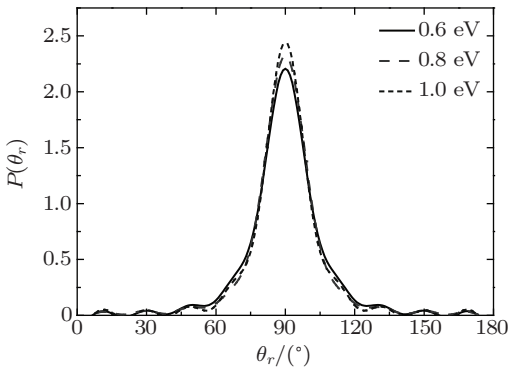


Fig. 2. Distributions of $P(\theta_r)$, reflecting the $\boldsymbol{k}$–$\boldsymbol{j}'$ correlation at three collision energies.

Comparing the dihedral angle distributions of the $\boldsymbol{k}$–$\boldsymbol{k}'$–$\boldsymbol{j}'$ correlation, which are calculated at three collision energies as shown in Fig. 3, one can realize some similar features. The distributions of $P(\phi_r)$ tend to be asymmetric about $\phi_r = 180^\circ$, directly reflecting the strong polarizations of angular momentum for the three reactions. For each reaction, the peak at $\phi_r = 270^\circ$ is evidently higher than that at $\phi_r = 90^\circ$, which reveals that the rotational angular momentum vector of product CaCl is not only aligned but also oriented along the negative direction of the y axis. It is very interesting that the peaks of the $P(\phi_r)$ distributions of the three reactions have the same trend; however there is a small discrepancy between three collision energies. The peak of $P(\phi_r)$ of the reaction at $E_T = 1.0$ eV is highest and that of the reaction at $E_T = 0.60$ eV is lowest at $\phi_r = 90^\circ$, and the peak of $P(\phi_r)$ of the reaction at $E_T = 0.8$ eV is highest and that of the reaction at $E_T = 1.0$ eV is lowest at $\phi_r = 270^\circ$. According to previous theoretical studies[41,42] about the molecular reaction for the reaction A + BC→AB + C, for the Ca + HCl→CaCl + H reaction, the angular momentum $\boldsymbol{j}'$ of the product molecule OH can be written as

$$j' = L\sin^2\beta + j\cos^2\beta + \boldsymbol{J}_1 m_{\mathrm{Cl}}/m_{\mathrm{CaCl}}, \tag{14}$$

$$\cos^2\beta = \frac{m_{\mathrm{Ca}} m_{\mathrm{H}}}{(m_{\mathrm{Ca}} + m_{\mathrm{cl}})(m_{\mathrm{cl}} + m_{\mathrm{H}})}, \tag{15}$$

$$J_1 = \sqrt{\mu_{\mathrm{HCl}} \boldsymbol{E}_R}\,(r_{\mathrm{CaCl}} \times \boldsymbol{r}_{\mathrm{HCl}})\,. \tag{16}$$

Here, $\boldsymbol{L}$ and $\boldsymbol{j}$ represent the reactant orbital momentum and rotational angular momentum, respectively; μ_{HCl} is the reduced mass of the HBr molecule; $\boldsymbol{E}_{\mathrm{R}}$ is the repulsive energy; and vectors $\boldsymbol{r}_{\mathrm{CaCl}}$ and $\boldsymbol{r}_{\mathrm{HCl}}$ are unit vectors, with Cl pointing to Ca and H, respectively. During the chemical-bond forming and breaking for the Ca + HCl reaction, the term $\boldsymbol{L}\sin^2\beta + \boldsymbol{J}\cos^2\beta$ in the equation is symmetric, while the term $\boldsymbol{J}_1 m_{\mathrm{Cl}}/m_{\mathrm{CaCl}}$ shows a preferred direction because of the effect of repulsive energy, which leads to the orientation of the CaCl product.

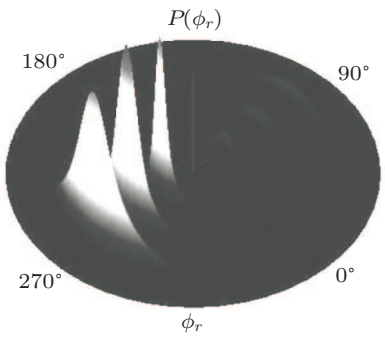


Fig. 3. $P(\phi_r)$ distributions, each as a function of the dihedral angle ϕ_r at three collision energies of 0.6, 0.8, and 1.0 eV (from inner to outer) for the Ca + HCl→CaCl + H reactions.

In order to obtain more detailed information about the reaction dynamics, we also plot the distributions of $P(\theta_r, \phi_r)$ in Fig. 4. Each of the three $P(\theta_r, \phi_r)$ distributions has two distinct peaks located at $(90°, 90°)$ and $(90°, 270°)$, respectively, which are in good accordance with the distributions of $P(\theta_r)$ and $P(\phi_r)$. Furthermore, one can also conclude from the distributions of $P(\theta_r, \phi_r)$ that the products are preferentially polarized in the direction perpendicular to the scattering plane, and the products of the reaction are mainly left-handed, rotating counter-clockwise in planes parallel to the scattering plane.

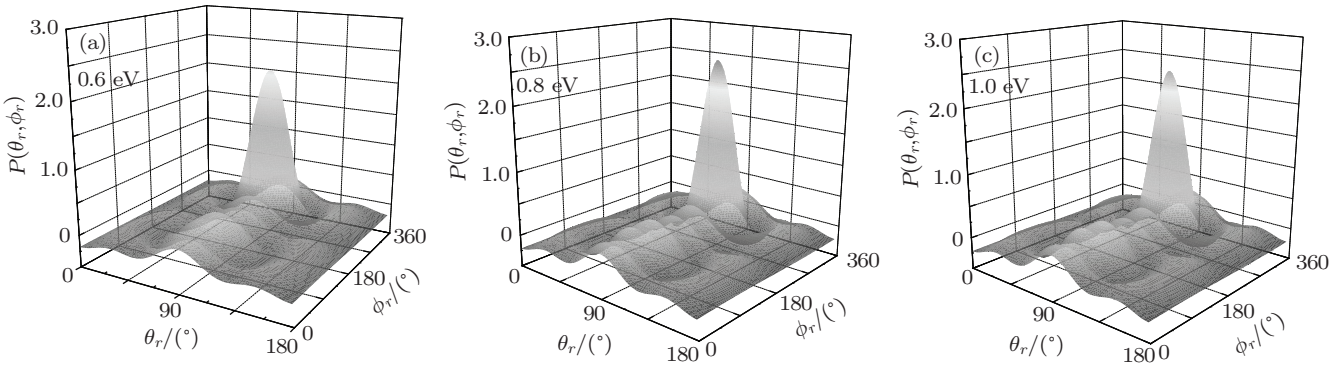


Fig. 4. Polar plots of $P(\theta_r, \phi_r)$ distribution averaged over all scattering angles, showing the distributions at collision energies of 0.6 eV (a), 0.8 eV (b), and 1.0 eV (c).

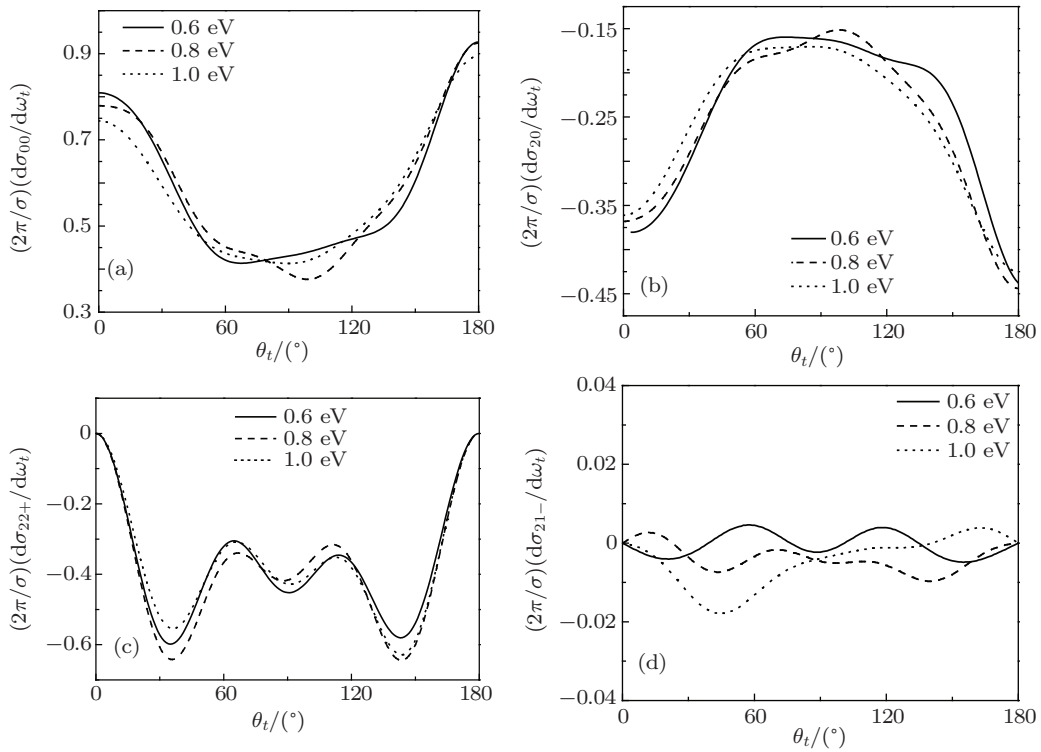


Fig. 5. (a) PDDCSs with $(k,q) = (0,0)$ (a), $(k,q\pm) = (2,0)$ (b), (2, 2+) (c), and (2, 1−) (d).

The polarization-dependent generalized PDDCSs describe the $\boldsymbol{k}$–$\boldsymbol{k}'$–$\boldsymbol{j}'$ correlation and the scattering direction of the product molecule. The results of the PDDSs for the title reaction at three collision energies are shown in Fig. 5(a). The PDDCS $(2\pi/\sigma)(d\sigma_{00}/d\omega_t)$, which is simply the differential cross section (DCS), only describes the $\boldsymbol{k}$–$\boldsymbol{k}'$ correlation or the scattering direction of the product and is not related to the orientation and alignment of the product rotational angular momentum vector $\boldsymbol{j}'$. It can be seen from Fig. 5(a) that the product is almost forwards and backwards scattering for the collision energy of 0.6 eV. With the increase in collision energy, the product is preferentially sideways and backward

scattering. The PDDCS $(2\pi/\sigma)(\mathrm{d}\sigma_{20}/\mathrm{d}\omega_t)$ is the expectation value of the second Legendre moment, which demonstrates the trend that is opposite to that of $((2\pi/\sigma)(\mathrm{d}\sigma_{00}/\mathrm{d}\omega_t))$, indicating that $\boldsymbol{j}'$ is strongly aligned along the direction perpendicular to $\boldsymbol{k}$. As can be seen from Fig. 5(b), at the extremities of the forward and backward scatterings, the PDDCSs with $q \neq 0$ are necessarily zero. At these limiting scattering angles, the $\boldsymbol{k}$–$\boldsymbol{k}'$ scattering plane is not determined and the values of these PDDCSs with $q \neq 0$ must be zero. The PDDCSs with $q \neq 0$ at the scattering angles away from the extremities of the forward and backward directions provide information about the ϕ_r dihedral angle distribution, and are nonzero at scattering angles away from $\theta_t = 0^\circ$ and 180°, for the sideways and backward scattering products. The distributions of the PDDCS $(2\pi/\sigma)(\mathrm{d}\sigma_{22+}/\mathrm{d}\omega_t)$ of the title reaction at three collision energies are shown in Fig. 5(c), and are relative to $\langle \sin^2\theta_r \cos^2\phi_r \rangle$. The value of $(2\pi/\sigma)(\mathrm{d}\sigma_{22+}/\mathrm{d}\omega_t)$ is negative for a majority of all scattering angles, indicating the remarkable preference of product alignment along the y axis. In particular, the product displays a stronger polarization at about 38° and 142°, respectively.

4. Conclusions

In the present paper, we employed the QCT method to study the product rotational polarizations of the Ca + HCl reaction at three collision energies ($E_\mathrm{T} = 0.6$, 0.8, and 1.0 eV) according to the PES of Verbockhaven *et al*. The results demonstrate that the rotational polarization of the product presents different characteristics for different collision energies. With the increase in collision energy, the product is preferentially sideways and backward scattering, and the peak of the $P(\theta_r)$ distribution of the product becomes higher. The product rotational angular momentum vector $\boldsymbol{j}'$ is not only aligned, but also oriented along the negative direction of the y axis. These characteristics may be ascribed to the HHL mass combination type and the construction of the PES. In a word, the effects of the collision energy on the vector property are not obvious, including the alignment, orientation, and PDDCSs.

Acknowledgment

All the calculations for the present study were carried out at the Shuguang 4000A Computer Center of Ludong University. Many thanks should be given to Prof. Han Ke-Li for providing the QCT code of the stereodynamics.

References

[1] Li H, Zheng B and Meng Q T 2012 *Acta Phys. Sin.* **61** 153401 (in Chinese)
[2] Zong F J, Han B R and Ji F 2012 *Chin. Phys. B* **21** 093103
[3] Xiao J, Yang C L and Wang M S 2012 *Chin. Phys. B* **21** 043101
[4] Chen X Q, Wang M S and Yang C L 2012 *Chin. Phys. B* **21** 023402
[5] Zhao J, Xu Y and Meng Q T 2010 *Chin. Phys. B* **19** 063403
[6] Xu Y, Zhao J, Wang J, Liu F and Meng Q T 2010 *Acta Phys. Sin.* **59** 3885 (in Chinese)
[7] Xiao J, Yang C L, Li X H, Wang M S and Ma X G 2011 *Chin. Phys. Lett.* **28** 013101
[8] Liang J J, Liu X G, Xu W W, Kong H and Zhong Q G 2010 *THEOCHEM* **942** 93
[9] Magee J L 1940 *J. Chem. Phys.* **8** 687
[10] Mims A, Lin S M and Hem R R 1972 *J. Chem. Phys.* **57** 3099
[11] Torres-Filho A and Pruett J G 1982 *J. Chem. Phys.* **77** 1774
[12] Cruse H W, Dagdigian P J and Zare R N 1973 *Faraday Discuss. Chem. Soc.* **55** 277
[13] Pruett J G and Zare R N 1976 *J. Chem. Phys.* **64** 1774
[14] Gupta A, Perry D S and Zare R N 1980 *J. Chem. Phys.* **76** 237
[15] Zare R N 1979 *Faraday Discuss. Chem. Soc.* **67** 7
[16] Feldman D, Lengel R and Zare R N 1977 *Chem. Phys. Lett.* **52** 413
[17] Cai M Q, Zhang L, Tang B Y, Chen M D, Yang G W and Han K L 2000 *Chem. Phys.* **283** 255
[18] Noda C, Mckillop J S, Johnson M A, Waldeck J R and Zare R N 1986 *J. Chem. Phys.* **85** 856
[19] Zhao D and Zare R N 1992 *J. Chem. Phys.* **97** 6208
[20] Tsekouras A A, Leach C A, Kalogerakis K S and Zare R N 1992 *J. Chem. Phys.* **97** 720
[21] Teule J M, Jassen M H N, Bulthuis J and Stolte S 1999 *J. Chem. Phys.* **110** 10792
[22] Altkom R, Bartoszek F E, Haven J D, Han G C, Perry D S and Zare R N 1983 *Chem. Phys. Lett.* **98** 212
[23] Karny Z, Estler R C and Zare R N 1979 *J. Chem. Phys.* **69** 5199
[24] Gupta A, Perry D S and Zare R N 1980 *J. Chem. Phys.* **72** 6250
[25] Karny Z and Zare R N 1978 *J. Chem. Phys.* **68** 3360
[26] Soep B, Whitham C J, Keller A and Visticot J P 1991 *Faraday Discuss. Chem. Soc.* **91** 191
[27] Soep B, Abbés S, Keller A and Visticot J P 1992 *J. Chem. Phys.* **96** 440
[28] Keller A, Lawruszczuk R, Soep B and Visticot J P 1996 *J. Chem. Phys.* **105** 4556
[29] Visticot J P, Soep B and Whitham C J 1988 *J. Phys. Chem.* **92** 4574
[30] Verbockhaven G, Sanz C, Groenenboom G C and Roncero O 2005 *J. Chem. Phys.* **122** 204307
[31] Wang L Z, Yang C L, Liang J J, Xiao J and Zhang Q G 2011 *Chin. J. Chem. Phys.* **24** 686
[32] Wang L Z, Yang C L, Liang J J, Duan L L and Zhang Q G 2012 *J. Chem. Phys.* **405** 181
[33] Han K L, He G Z and Lou N Q 1996 *J. Chem. Phys.* **105** 8699
[34] Wang M L, Han K L and He G Z 1998 *J. Chem. Phys.* **109** 5446
[35] Wang M L, Han K L and He G Z 1998 *J. Phys. Chem. A* **102** 10204
[36] Zhang X and Han K L 2006 *Int. J. Quantum Chem.* **106** 1815
[37] Zhang W Q, Cong S L, Zhang C H, Xu X S and Chen M D 2009 *J. Phys. Chem. A* **113** 4192
[38] Zhang W Q, Li Y Z, Xu X S and Chen M D 2010 *Chem. Phys.* **367** 115
[39] Aoiz F J, Brouard M and Enriquez P A 1996 *J. Chem. Phys.* **105** 4964
[40] Ma J J, Chen M D, Cong S L and Han K L 2006 *Chem. Phys.* **327** 529
[41] Li R J, Han K L, Li F E, Lu R C, He G Z and Lou N Q 1994 *Chem. Phys. Lett.* **220** 286
[42] Han K L, Zhang L, Xu D L, He G Z and Lou N Q 2001 *J. Phys. Chem. A* **105** 2956